Journal of the European Ceramic Society **15** (1995) 661–666
© 1995 Elsevier Science Limited
Printed in Great Britain. All rights reserved
0955-2219/95/$9.50

0955-2219(95)00039-2

Some Properties of Aluminium-Nitride Powder Prepared by Metal–Organic Chemical Vapour Deposition

Kazuro Kubo, Kiyoshi Itatani,* F. Scott Howell, Akira Kishioka & Makio Kinoshita

Department of Chemistry, Faculty of Science and Engineering, Sophia University, 7–1 Kioi-cho, Chiyoda-ku, Tokyo 102, Japan

(Received 29 September 1994; revised version received 2 February 1995; accepted 7 February 1995)

Abstract

Ultrafine aluminium-nitride (AlN) powders with primary particle sizes of 10–20 nm were prepared by a metal–organic chemical vapour deposition (MOCVD): trimethylaluminium ($Al(CH_3)_3$), triethylaluminium ($Al(C_2H_5)_3$) and triisobutylaluminium ($Al(i\text{-}C_4H_9)_3$)-vapours were reacted with ammonia (NH_3) at 1050°C. The sintered compacts with relative densities of ~95% could be fabricated by firing these compressed powders at temperatures as low as 1600°C. The relative densities of the $Al(CH_3)_3$-derived and $Al(C_2H_5)_3$-derived compacts fired at 1800°C for 10 h attained ~98%. The oxygen contents of these compacts were 1·8 and 4·7%, respectively.

1 Introduction

Aluminium-nitride (AlN) ceramics have high thermal conductivities (theoretical value; 320 $Wm^{-1} \times K^{-1}$)[1] and low thermal expansion coefficients (4·4 $\times 10^{-6}$°C^{-1}; 25–400°C) close to that of silicon.[2] By making use of these properties, AlN ceramics have started to be used as a high-performance ceramic substrate and packaging material. To date, (i) the preparation of high-purity AlN powder and (ii) the fabrication of high-density AlN ceramics with and without a sintering aid have been examined by many researchers.

The high-purity AlN powder may be prepared either by a direct nitridation of metallic aluminium (Al) or by a carbothermal reduction of Al_2O_3.[2,3] Recently, much attention is being devoted to the preparation of high-purity and ultrafine AlN powder by a chemical vapour deposition (CVD), because this AlN powder has a potential application in the fabrication of high-density AlN ceramics without a sintering aid. Various vapourization sources have been proposed by many researchers: metallic Al,[4–8] aluminium chloride ($AlCl_3$)[9–13] and alkylaluminium.[14–16] Among these sources, the vapourization rate of alkylaluminium may be controlled more strictly than those of solid sources, because the commercially available alkylaluminiums: trimethylaluminium ($Al(CH_3)_3$: TMAL), triethylaluminium ($Al(C_2H_5)_3$): TEAL) and triisobutylaluminium ($Al(i\text{-}C_4H_9)_3$: TIBAL) are not solid but liquid at room temperature. The properties of TEAL-derived AlN powder have been reported by Wakimura and Hiai,[15] and Adjaottor and Griffin;[16] those of TIBAL-derived AlN powder by Tsuchida *et al.*[14] But the properties, especially sinterabilities, of AlN powders prepared by the vapour-phase reactions of alkylaluminiums with ammonia (NH_3) have never been examined systematically.

The present authors[8] have examined the properties of AlN powder prepared by a low-pressure CVD (LP-CVD), using metallic Al and NH_3–nitrogen (N_2) gas. This paper deals with: (i) the preparation of AlN powder by a metal organic CVD (MOCVD); (ii) the evaluation of the powder properties and (iii) the comparison of the present data with those of our previous LP-CVD.

2 Experimental Procedure

2.1 Starting materials and reaction apparatus

Three kinds of alkylaluminiums available from Aldrich Chemical Company (Milwaukee, WI, USA) were used as starting materials: (i) TMAL; (ii) TEAL and (iii) TIBAL.

The schematic diagram of the reaction apparatus assembled by ourselves is shown in Fig. 1. The apparatus consisted of: (i) a reacting zone ((a)–(e)); (ii) a collecting zone ((f)–(h)), and (iii) an evacuating

---

*To whom correspondence should be addressed.

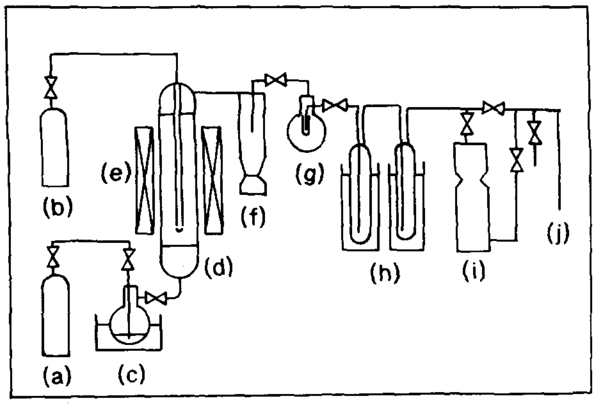

Fig. 1. Schematic diagram of the reaction apparatus: (a) N_2 cylinder (purity: 99·9995%); (b) NH_3 cylinder (purity: 99·99%); (c) Evaporation flask; (d) Mullite tube (diameter: 3 cm, height: 60 cm); (e) Electric furnace (heating zone: 30 cm); (f) Cyclone; (g) Test-tube type filter; (h) Trap; (i) Oil-diffusion pump and (j) Rotary pump.

Table 1. Preparation conditions of AlN powders

	(Evaporation)	*(Flow rate)*	
Alkylaluminium	*Temperature (°C)*	*NH_3 gas (dm^3 min^{-1})*	*Carrier gas (N_2) (dm^3 min^{-1})*
$Al(CH_3)_3$	30	50–100	50
$Al(C_2H_5)_3$	110	50	50–100
$Al(i\text{-}C_4H_9)_3$	100	50	100–200

zone ((i)–(j)). The reaction apparatus was first evacuated using the rotary and oil-diffusion pumps. Then alkylaluminium vapour with the partial pressure of 15 mmHg, which was formed by controlling the heating temperature of the liquid alkylaluminium, was introduced into the reaction tube heated at 1050°C, using a carrier gas of nitrogen (N_2) with purity of over 99·9995%; NH_3 gas with purity of 99·99% was simultaneously introduced into the reaction tube. The evaporation conditions of alkylaluminium and the flow rates of NH_3 and N_2 are listed in Table 1. The resulting powder was collected by a cyclone filter and a test-tube type filter. The yield of the powder was ~80% of the theoretical yield.

2.2 Phase identification and quantitative analysis

The crystalline phase of the resulting powder was examined using an X-ray diffractometer with CuKα_1 radiation operated at 40 kV and 25 mA (Model Rad IIA, Rigaku, Tokyo). The aluminium content of the resulting powder was determined using an X-ray fluorescence apparatus (Model SXF-1200, Shimadzu, Kyoto); the nitrogen and oxygen contents were determined using a simultaneous nitrogen/oxygen analyser (Model EMGA-550, Horiba, Kyoto).

2.3 Evaluation of powder properties

The specific surface area of the resulting powder was measured by BET technique, using nitrogen (N_2) as an adsorption gas. The particle shape was observed using a transmission electron microscope (TEM; Model H-800; accelerating voltage 200 kV, Hitachi, Tokyo). The particle-size distribution was measured by a laser scattering/diffraction apparatus (Model LA-700, Horiba, Kyoto).

2.4 Evaluation of sinterability

Two kinds of the compacts were fabricated to evaluate the sinterability of the resulting powder; each compact with a diameter of 10 mm and thickness of 10 mm for the dilatometric evaluation was fabricated by pressing ~1·3 g of the powder uniaxially at 50 MPa; each compact with a diameter of 10 mm and thickness of ~3 mm for the measurement of density and microstructural observation was fabricated by pressing ~0·3 g of the powder uniaxially at 50 MPa.

The densification behaviour of the compact was evaluated using a dilatometer from room temperature up to ~1600°C at the heating rate of 5°C min^{-1}. The relative density (bulk density/true density) of the compact fired at a temperature between 1400 and 1800°C for 3 or 10 h, in N_2 flowing at the rate of 2 dm^3 min^{-1}, was calculated using the data on dimensions and weight of the compact; the heating rate from room temperature up to the desired temperatures was 10°C min^{-1}. The fractured surfaces of the sintered compact were observed using a scanning electron microscope (SEM; Model S-430, Hitachi, Tokyo).

3 Results and Discussion

3.1 Crystalline phase of the resulting powder

The powders were deposited not only on the walls (upper parts) of the reaction tube but also on the cyclone and test-tube type filter. The resulting powders were white.

Typical XRD patterns of the powders collected from the cyclone and filter are shown in Fig. 2. Only AlN[17] was detected from the powders, irrespective of the difference in the kind of alkylaluminium. The crystallinities of these powders were almost the same as those collected from the cyclone and filter.

The analytical results of the present powders are listed in Table 2. The molar ratios of Al to N were in the range of 1·00–1·08. The oxygen content varied from 4·6 to 9·9%, according to the kind of alkylaluminium.

The reaction routes of TMAL, TEAL and TIBAL with NH_3 have been examined by several researchers.[14,15,18] Details will be described below:

(i) Reaction route of TMAL with NH_3[18]

$$Al(CH_3)_3 + NH_3 \rightarrow Al(CH_3)_3{\cdot}NH_3 \qquad (1)$$

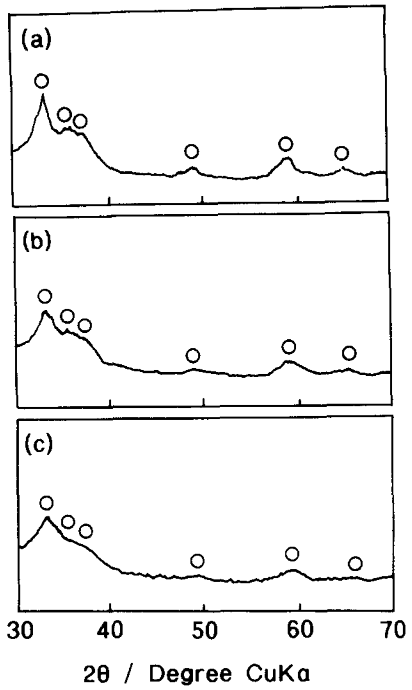

Fig. 2. X-ray diffraction patterns of (a) TMAL-derived powder; (b) TEAL-derived powder and (c) TIBAL-derived powder. ○ AlN — Reaction temperature: 1050°C.

Table 2. Analytical results of the powders and molar ratios of Al to N. Reaction temperature: 1050°C

Alkylaluminium	*Al (wt%)*	*N (wt%)*	*O (wt%)*	$\frac{Al}{N}$
$Al(CH_3)_3$	63·5	31·9	4·6	1·03
$Al(C_2H_5)_3$	61·1	31·7	7·2	1·00
$Al(i\text{-}C_4H_9)_3$	61·0	29·1	9·9	1·08

$$Al(CH_3)_3{\cdot}NH_3 \rightarrow Al(CH_3)_2NH_2 + CH_4 \qquad (2)$$
$$Al(CH_3)_2NH_2 \rightarrow AlCH_3NH + CH_4 \qquad (3)$$
$$AlCH_3NH \rightarrow AlN + CH_4 \qquad (4)$$

(ii) Reaction route of TEAL with NH_3[15]

$$Al(C_2H_5)_3 + NH_3 \rightarrow Al(C_2H_5)_2{\cdot}NH_2 + C_2H_6 \qquad (5)$$
$$Al(C_2H_5)_2{\cdot}NH_2 \rightarrow (1/n)\,(AlC_2H_5NH)_n + C_2H_6 \qquad (6)$$
$$(AlC_2H_5NH)_n \rightarrow nAlN + C_2H_6 \qquad (7)$$

(iii) Reaction route of TIBAL with NH_3[14]

$$Al(i\text{-}C_4H_9)_3 + NH_3 \rightarrow Al(i\text{-}C_4H_9)_3{\cdot}NH_3 \qquad (8)$$
$$Al(i\text{-}C_4H_9)_3{\cdot}NH_3 \rightarrow AlN + 3(i\text{-}C_4H_{10}) \qquad (9)$$

The upsurges of the X-ray baseline spectra in the range of 30–40° suggest the presence of some amorphous material. The composition of such amorphous material appears to be Al–O–N system, partly because 4·6–9·9% of oxygen are included in the powder, and partly because Al/N ratios above unity indicate somewhat lower nitrogen contents than stoichiometry.

The oxygen may come to be included in the powder during the handling in air.[19] The present oxygen contents (4·6–9·9%) are, however, much smaller than those reported previously; the previous data showed that TEAL-derived and TIBAL-derived powders contain 15–20% of oxygen.[14–16]

3.2 Powder properties

The properties of the resulting powders were examined from the viewpoints of specific surface area, particle shape and particle size.

The specific surface areas of the resulting powders were arranged in the following order: TIBAL-derived powder (175 m^2g^{-1}) > TEAL-derived powder (145 m^2g^{-1}) > TMAL-derived powder (95 m^2g^{-1}). The primary particle sizes calculated on the basis of the surface areas were arranged as follows: TMAL-derived powder (19 nm) > TEAL-derived powder (13 nm) > TIBAL-derived powder (11 nm).

The TEM micrographs and histograms for particle-size distributions of the resulting powders are shown in Fig. 3. The TEM micrographs of TMAL-derived and TEAL-derived powders (Fig. 3(a) and (b)) showed that the polyhedral particles with sizes of $<0{\cdot}05$ μm (50 nm) were adhered to form agglomerates; the histograms for the particle-size distribution indicated that the particles with sizes of $<0{\cdot}5$ μm and with sizes of 1 to 30 μm were present in the powder. The TEM micrograph of TIBAL-derived powder (Fig. 3(c)) showed that the polyhedral particles with sizes of $<0{\cdot}05$ μm (50 nm) were linked to form agglomerates; the histogram for the particle-size distribution revealed that the particle sizes were distributed in the ranges of 0·1–0·2 μm and of 2–30 μm.

The individual particles observed by TEM correspond to primary particles, because the particle

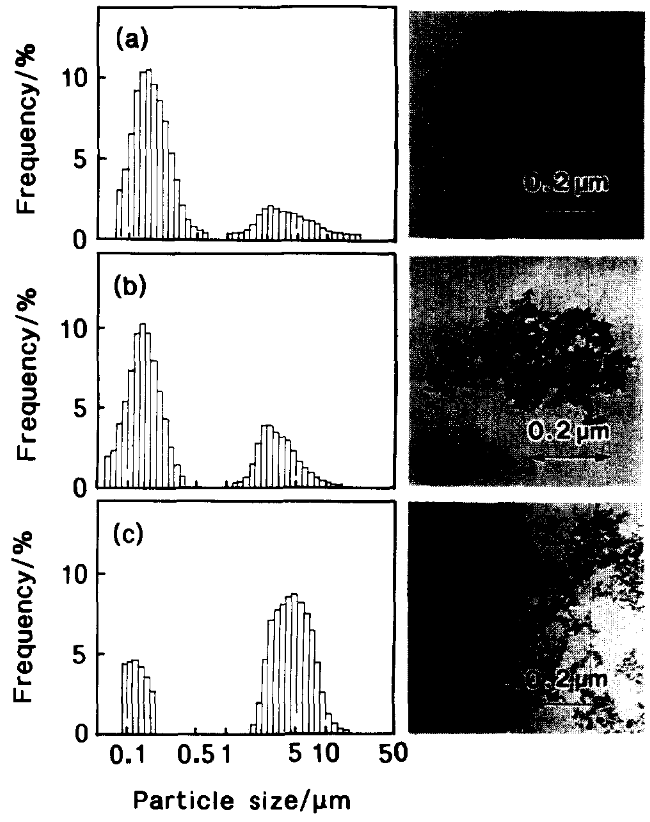

Fig. 3. Particle-size distributions and TEM micrographs of (a) TMAL-derived powder; (b) TEAL-derived powder and (c) TIBAL-derived powder.

sizes (< 50 nm) observed by TEM are in accord with the primary particle sizes of 10–20 nm. These primary particle sizes are smaller than those (30–50 nm) prepared by LP-CVD[8] and those (20–80 nm) by rf plasma.[6]

The particles with sizes of < 0·5 μm correspond to secondary particles where the primary particles are adhered to one another; the particles with sizes of 1–30 μm correspond to ternary particles which are formed by the agglomeration of the secondary particles. The secondary and ternary particles may form spontaneously to lower the excess surface energy which the ultrafine primary particles possess.

3.3 Sinterability

Before we fabricated the high-density AlN ceramics, we examined the linear shrinkages of these compacts during heating. Results are shown in Fig. 4. The shrinkage of TMAL-derived compact proceeded with temperature and was promoted at temperature exceeding 1200°C. The shrinkage of TEAL-derived compact was similar to that of TMAL-derived compact but was slightly shifted toward the higher temperature side. The shrinkage of TIBAL-derived compact started to occur at ~200°C and was promoted above 1400°C.

The shrinkages during the heating of TMAL-derived and TEAL-derived compacts below ~1200°C and during the heating of TIBAL-derived compact below ~1400°C may be attributed to (i) the elimination of residual carbon formed by the decomposition of alkyl groups and (ii) the elimination of oxygen and H_2O adsorped on the AlN particles. The weight loss (~10%) of TIBAL-derived compact before and after the dilatometric measurement is more appreciable than the weight losses (~5%) of TMAL-derived and TEAL-derived compacts.

As shown above, the rapid shrinkages during the heating of these three compacts above 1200–1400°C indicate the initiation of the mass transfer due to the sintering of AlN particles. On the basis of this information, we decided to fire the compacts at 1400°C or at a higher temperature. The relationship between firing temperature and relative density is shown in Fig. 5. The relative densities for these compacts varied from 60 to 67% at the firing temperature of 1400°C; however, they increased with increasing temperature and attained 95–96% at and above 1600°C.

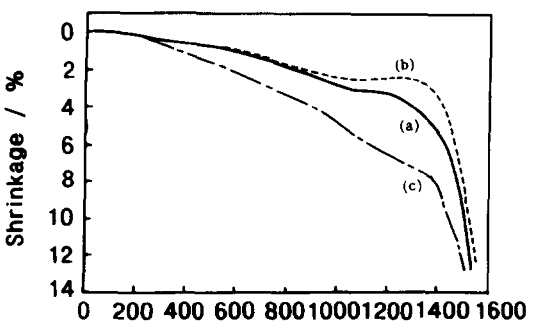

Fig. 4. Expansion-shrinkage curves of (a) TMAL-derived compact; (b) TEAL-derived compact and (c) TIBAL-derived compact. Heating rate: 5°C min^{-1}.

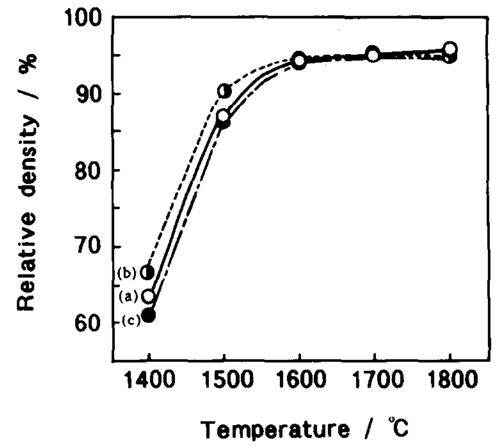

Fig. 5. Effect of firing temperature on the relative density of the compact. (a) TMAL-derived compact; (b) TEAL-derived compact and (c) TIBAL-derived compact. Heating rate: 5°C min^{-1}.

Although the sintering temperatures of the conventional pure AlN powders with the surface areas of 1–5·3 m^2g^{-1} usually need to be 1850°C or higher,[2,20] those of the present AlN powders with the surface areas of 95–175 m^2g^{-1} are as low as 1600°C. This sintering temperature is in accord with that of AlN powder with the surface area of 92 m^2g^{-1} prepared by rf plasma.[6] Thus, the difference in sintering temperature between conventional pure and present ultrafine AlN powders can be attributed to the surface area or the primary particle size. Moreover, the oxygen in AlN powder may create the cation vacancies to promote the mass transfer during sintering;[19] however, Kuramoto and his coworkers[2,20] state that the particle-size effect, i.e. small particle size and narrow particle-size distribution, contributes much more to the densification of the AlN compact than the oxygen effect does. In actual fact, the relative densities of these sintered compacts are all in the range of 95–96% at and above 1600°C, regardless of the differences in oxygen contents among the starting powders.

The crystalline phases of the compacts fired at 1800°C for 3 h were examined by XRD. Although the data were omitted in this paper, the XRD patterns of these sintered compacts showed that the crystalline phases were not only AlN but also $Al_{(8/3+x/3)}O_{4-x}N_x$[21] (trace).

The oxynitride or $Al_{(8/3+x/3)}O_{4-x}N_x$ results from the reaction of AlN with H_2O and/or O_2 during firing. Although the sintering of AlN powder is promoted by the presence of oxygen,[2] the thermal

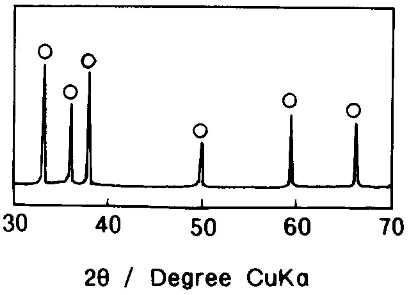

Fig. 6. Typical X-ray diffraction pattern of TMAL-derived compact. ○ AlN — Firing conditions: 1800°C for 10 h.

Table 3. Some properties of the compact fired at 1800°C for 10 h.

Alkylaluminium	*Relative density (%)*	*Phase*[a]	*Oxygen (%)*
$Al(CH_3)_3$	97·9	AlN	1·8
$Al(C_2H_5)_3$	98·2	AlN	4·7
$Al(i\text{-}C_4H_9)_3$	95·1	AlN	5·2

[a] Identified by X-ray diffractometry.

conductivity lowers with increasing oxygen content.[2,22] The oxygen content may be reduced by firing the compact in nitrogen atmosphere.[23] In order to: (i) reduce $Al_{(8/3+x/3)}O_{4-x}N_x$ content and (ii) increase the relative density over ~95%, the firing time was prolonged from 3 to 10 h at the fixed temperature of 1800°C. We examined the crystalline phases of the compacts by XRD. As a typical case, the XRD pattern of TMAL-derived compact is shown in Fig. 6. Only AlN was detected from the sintered compact.

The relative density, crystalline phase and oxygen content are listed in Table 3. The relative density of TIBAL-derived compact was limited to be 95·1%; however, the relative densities of TMAL-derived and TEAL-derived compacts attained ~98%. The crystalline phase was only AlN. The oxygen contents were in the range of 1·8–5·2%.

The SEM micrographs of these sintered compacts are shown in Fig. 7. The SEM micrographs of TMAL-derived and TEAL-derived compacts (Fig. 7(a) and (b)) showed that the grains with sizes of 1–4 μm were closely arrayed. The SEM micrograph of TIBAL-derived compact (Fig. 7(c)) showed that the grains with sizes of < 1 μm were present among the grains with sizes of 2–4 μm.

The fabrication of high-density AlN ceramics without a sintering aid has been examined chiefly by Kuramoto and his coworkers: the relative density of AlN compact fired at 2000°C for 3 h is 93%;[2] the firing of doctor-bladed powder compact at 1850°C for 7 h raises the relative density to 98·7%.[20] Since the relative densities of TMAL-derived and TEAL-derived compacts achieve ~95% at 1600°C for 3 h and ~98% at 1800°C for 10 h, these AlN powders prove to have excellent sinterabilities.

The SEM micrographs (Fig. 7) shows that the uniform-sized grains are closely arrayed, reflecting the high densities (95–98%) of the sintered compacts. Such microstructures demonstrate that the homogenous sintering may proceed among the ultrafine, uniform-sized and weakly-agglomerated AlN particles.[20]

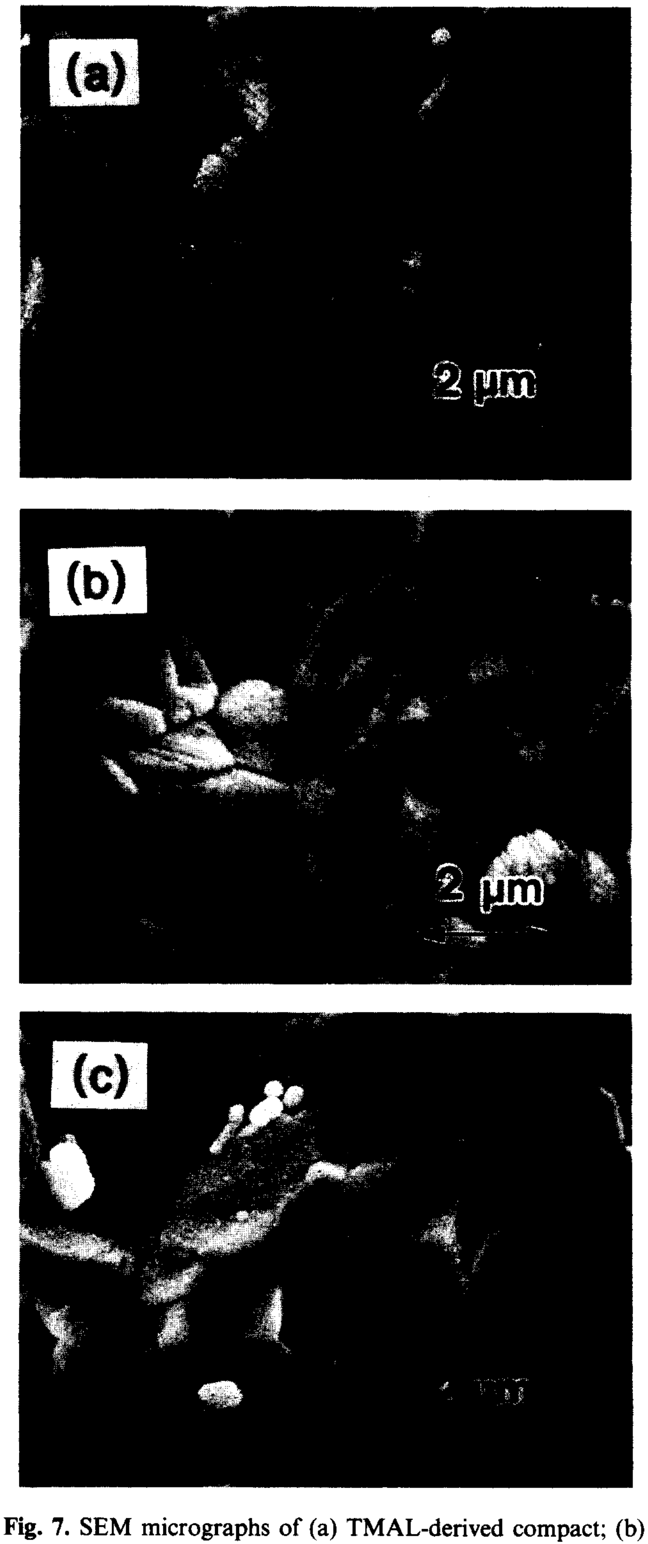

Fig. 7. SEM micrographs of (a) TMAL-derived compact; (b) TEAL-derived compact and (c) TIBAL-derived compact. Firing conditions: 1800°C, 10 h.

4 Conclusion

The aluminium-nitride (AlN) powders were prepared by the metal–organic chemical vapour deposition (MOCVD), i.e. the vapour-phase reactions of trimethylaluminium ($Al(CH_3)_3$: TMAL), triethylaluminium ($Al(C_2H_5)_3$: TEAL) and triisobutylaluminium ($Al(i\text{-}C_4H_9)_3$: TIBAL) with ammonia (NH_3). The properties of the resulting powders are summarized as follows:

(1) The specific surface areas of the resulting powders were 95–175 m^2g^{-1}; the primary particle sizes were in the range of 10–20 nm.
(2) The sintered compacts with the relative densities of ~95% could be fabricated by firing these powders at temperatures as low as 1600°C. When these compacts were fired at 1800°C for 10 h, the relative densities were 98·2% (TEAL-derived compact) > 97·9% (TMAL- derived compact) > 95·1% (TIBAL-derived compact).
(3) After the firing of the compacts at 1800°C for 10 h, only AlN was detected from the sintered compacts; the oxygen contents were 1·8% (TMAL-derived compact) < 4·7% (TEAL-derived compact) < 5·2% (TIBAL-derived compact).

Acknowledgements

The authors wish to express their thanks to Mr K. Nishinaka of Mitsubishi Materials Co. Ltd. for taking the TEM micrographs and to Dr T. Rouxel of Laboratoire de Matériaux Céramiques et Traitements de Surface of U.R.A.—CNRS 320 (France) for dilatometric measurements.

References

1. Borom, M. P., Slack, G. A. & Szymaszek, J. W., Thermal conductivity of commercial aluminum nitride. *Bull. Am. Ceram. Soc.*, **51** (1972) 852–6.
2. Kuramoto, N., Taniguchi, H. & Aso, I., Development of translucent aluminum nitride ceramics. *Am. Ceram. Soc. Bull.*, **68** (1989) 883–7.
3. Mroz, T. J., Aluminum nitride. *Am. Ceram. Soc. Bull.*, **71** (1992) 782, 84.
4. Matsumoto, O., Formation of aluminum nitride by use of a transferred plasma torch. *J. Electrochem. Soc. Jpn.*, **36** (1968) 207–12.
5. Uda, M., Ohno, S. & Okuyama, H., Preparation of ultrafine powders of AlN and (AlN + Al) by nitrogen plasma–Al reaction. *Yogyo-Kyokai-Shi*, **95** (1987) 86–90.
6. Baba, K., Shohata, N. & Yonezawa, M., Synthesis and properties of ultrafine AlN powder by rf plasma. *Appl. Phys. Letters*, **54** (1989) 2309–11.
7. Yokota, M., Yagyu, S., Majima, K. & Nagai, H., Preparation of ultra-fine aluminum nitride by gas phase reaction. *J. Powder and Powder Metall.*, **38** (1991) 382–5.
8. Itatani, K., Sano, K., Howell, F. S., Kishioka, A. & Kinoshita, M., Some properties of aluminium nitride powder synthesized by low-pressure chemical vapour deposition. *J. Mater. Sci.*, **28** (1993) 1631–8.
9. Kimura, I., Hotta, N., Nukui, H., Saito, N. & Yasukawa, S., Synthesis of fine AlN powder by vapour phase reaction of $AlCl_3$ and NH_3, *J. Ceram. Soc. Jpn.*, **96** (1988) 206–10.
10. Nickel, K. G., Riedel, R. & Petzow, G., Thermodynamic and experimental study of high-purity aluminum nitride formation from aluminum chloride by chemical vapor deposition. *J. Am. Ceram. Soc.*, **72** (1989) 1804–10.
11. Riedel, R. & Gaudl, K. -U., Formation and characterization of amorphous aluminum nitride powder and transparent aluminum nitride film by chemical vapor deposition. *J. Am. Ceram. Soc.*, **74** (1991) 1331–4.
12. Park, J. -R., Rhee, S. -W. & Lee, K. -H., Gas-phase synthesis of AlN powders from $AlCl_3$–NH_3–N_2. *J. Mater. Sci.*, **28** (1993) 57–64.
13. Greil, P., Kulig, M., Hotza, D., Lange, H. & Tischtau, R., Aluminium nitride ceramics with high thermal conductivity from gas-phase synthesized powders. *J. Eur. Ceram. Soc.*, **13** (1994) 229–37.
14. Tsuchida, K., Takeshita, Y., Yamane, A. & Kato, A., Preparation of AlN powders by vapor phase reaction of $Al(i\text{-}Bu)_3$–NH_3 system. *Yogyo-Kyokai-Shi*, **95** (1987) 1198–1201.
15. Wakimura, K. & Hiai, A., AlN powders produced by vapour phase reaction from aluminum alkyl. *Function and Materials*, **11**(2) (1991) 13–9.
16. Adjaottor, A. A. & Griffin, G. L., Aerosol synthesis of aluminum nitride powder using metalorganic reactants. *J. Am. Ceram. Soc.*, **75** (1992) 3209–14.
17. Powder Diffraction File Card No. 25-1133, JCPDS International Center for Diffraction Data, Swarthmore, PA, USA, 1975.
18. Interrante, L. V., Carpenter II, L. E., Whitmarsh, C., Lee, W., Garbauskas, M. & Slack, G. A., Studies of organometallic precursors to aluminum nitride. *Mat. Res. Soc. Symp. Proc.*, **73** (1986) 359–66.
19. Sakai, T. & Iwata, M., Effect of oxygen on sintering of AlN. *J. Mater. Sci.*, **12** (1977) 1659–65.
20. Kuramoto, N., Aluminum nitride powder and its situation. *Bull. Ceram. Soc. Jpn.*, **22** (1987) 29–34.
21. Powder Diffraction File Card No. 18-52. JCPDS International Center for Diffraction Data, Swarthmore, PA, USA, 1968.
22. Slack, G. A., Nonmetallic crystals with high thermal conductivity. *J. Phys. Chem. Solids*, **34** (1973) 321–35.
23. Sato, T. & Iwata, M., Preparation of aluminum nitride by electric arc method. *Nippon Kagaku Kaishi*, **1973** (1973) 1869–73.